【C型肝炎と酸化ストレス】

Oxidative stress in chronic hepatitis C

日野 啓輔[1)]・古谷 隆和[2)]・是永 匡紹[2)]

Hino Keisuke Furuya Takakazu Korenaga Masaaki

Key words
mitochondria, iron, alcohol

要 約

C型肝炎は同じウイルス性肝炎であるB型肝炎とは病態が異なる部分も多く，その原因のひとつとして酸化ストレスの関与が挙げられる。最近の研究からC型肝炎における酸化ストレスの発生機序が次第に明らかになりつつある。コア蛋白はミトコンドリアの電子伝達系，とくに呼吸鎖複合体Ⅰの機能障害を引き起こすことで活性酸素を産生させやすくすることがひとつの機序と考えられる。しかし，HCV蛋白自体による酸化ストレスのmagnitudeはそれほど大きいものではなく，臨床的にはHCV感染の経過を修飾する二次的な酸化ストレスの関与が重要となる。HCV蛋白存在下ではアルコールや肝内鉄過剰などのストレスに対する感受性が亢進しており，これらの酸化ストレス因子はHCV蛋白と相乗的にミトコンドリア障害を引き起こし，肝病変を進展させ，最終的には肝腫瘍の発生を促進することが明らかとなった。したがって，これからのC型肝炎の治療はウイルス排除に加えて，いかに酸化ストレスを抑えていくかが重要な課題となる。

はじめに

C型肝炎では一般的に加齢とともに肝炎の活動性が強くなる傾向にあり，同じウイルス性肝炎であるB型肝炎とは逆の現象が見られる。また，肝発癌率もC型肝炎はB型肝炎の約7倍にも達し，こうした相違は両者の病態に起因すると考えられる。C型肝炎の病態に酸化ストレスが重要な役割を果たすことは広く知られているが，最近の知見からC型肝炎における酸化ストレスの発生機序も次第に明らかになりつつある。本稿では自検例を交えてC型肝炎における酸化ストレスの発生機序とその意義について考察する。

1. HCVコア蛋白と酸化ストレス

HCV構造蛋白の一つであるコア蛋白はin vivoやin vitroの系で酸化ストレスを誘導することが明らかにされている[1,2]。コア遺伝子導入マウスでは還元型グルタチオン（GSH）の低下や加齢による肝内過酸化脂質の増加が報告されている[1]。コア蛋白を発現する培養細胞でも活性酸素や過酸化脂質が上昇し，抗酸化反応因子の遺伝子発現が誘導されることから，これらの現象がコア蛋白により直接に引き起こされていると考えられる[3]。では，コア蛋白による活性酸素の産生部位はどこであろうか。これまでにコア蛋白の細胞内局在部位として小胞体，脂肪滴，ミトコンドリアなどが報告されているが，われわれはミトコンドリアが細胞内の活性酸素の最大産生部位であることに注目して，コア蛋白がミトコンドリアに及ぼす影響についてHCV構造蛋白発現マウスや精製コア蛋白を用いて検討を行った[3]。

その結果，コア蛋白がミトコンドリア外膜に結合し，呼吸鎖複合体Ⅰの機能障害を引き起こすことで，活性酸素の産生が増強することを明らかにした。これらの結果はコア蛋白がミトコンドリア外膜と小胞体との間（mitochondria associated membrane）に存在するという報告[4]ともよく一致した。一方，コア

[1)]山口大学大学院医学系研究科基礎検査学：Department of Basic Laboratory Sciences, Yamaguchi University Graduate School of Medicine [2)]山口大学大学院医学系研究科消化器病態内科学：Department of Gastroenterology and Hepatology
〒755-8505 山口県宇部市南小串1-1-1 FAX：0836-22-2130 E-mail：k.hino@yamaguchi-u.ac.jp

表　鉄負荷HCVトランスジェニックマウスにおける肝腫瘍発生率（文献7から引用）

Feeding period	Mice	Number of mice	Liver tumor
6 months	nonTgM-C	10	0/10
	TgM-C	10	0/10
	nonTgM-Fe	10	0/10
	TgM-Fe	10	0/10
9 months	nonTgM-C	7	0/7
	TgM-C	6	0/6
	nonTgM-Fe	5	0/5
	TgM-Fe	6	0/6
12 months	nonTgM-C	10	0/10
	TgM-C	8	0/8
	nonTgM-Fe	9	0/9
	TgM-Fe	11	5/11

nonTgM-C；通常餌飼育コントロールマウス　TgM-C；通常餌飼育トランスジェニックマウス　nonTgM-Fe；鉄過剰餌飼育コントロールマウス　TgM-Fe；鉄過剰餌飼育トランスジェニックマウス

蛋白の発現調節が可能な培養細胞を極少量のtBOOHで刺激し，位相差顕微鏡で活性酸素センサーである蛍光色素を観察したところミトコンドリアより徐々に染まるのが確認された[6]。このようにコア蛋白による活性酸素部位として，ミトコンドリアが重要であることは明らかであるが，ミトコンドリア以外の可能性についても今後の検討が必要である。

2.　酸化ストレス感受性の亢進

コア蛋白発現マウスでの肝発癌に示されるように[7]，コア蛋白による直接的酸化ストレスが，C型肝炎の病態形成に重要であることは明らかである。しかし，in vitroの検討からも明らかなようにコア蛋白自体による酸化ストレスのmagnitudeは決して大きいものではない[8]。臨床的にみてもHCV感染者が一様に肝硬変へ進展したり肝発癌を来たしたりするわけではなく，HCV感染に加えたアルコール，加齢，鉄過剰などの二次的な酸化ストレスが病態の進行に密接に関与すると考えられる。それではHCV蛋白により引き起こされる酸化ストレスとは別に，HCV蛋白存在下では酸化ストレスに対する感受性も亢進しているのであろうか。この点についてアルコールと鉄過剰の2点から考察を行う。

アルコールが酸化ストレスに及ぼす機序としては，①アルコール脱水素酵素やアルデヒド脱水素酵素はNADからNADHへの変換を促進し，NADHはミトコンドリア電子伝達系への直接的なdonorであり，ミトコンドリアの呼吸鎖が過剰反応することで活性酸素が産生される。②アルコールがミトコンドリア膜に作用し，細胞質からミトコンドリアへのGSHの移動を阻害することによりミトコンドリア内の抗酸化能が低下する。③アルコールの代謝に関与するcytochrome 2E1 (CYP2E1)が慢性的なアルコール接種によりさらに誘導され，その増加が活性酸素の産生を亢進することが報告されている。そこで，アルコール摂取により誘導されるCYP2E1が，コア蛋白による酸化ストレスを増強するか否かについて検討した[9]。コア蛋白の発現調節が可能な培養細胞にCYP2E1をstable transfectionし，コントロール，HCV感染者，飲酒家，HCV＋飲酒家のモデルを作成した。HCV＋飲酒家モデル，すなわちコア蛋白＋CYP2E1発現細胞は，それぞれ単独発現に比べて相乗的に活性酸素の産生を増大させた。それに伴い細胞死も増加し，アルコールはHCVによる酸化ストレスを増大させ肝障害を悪化させていることが明らかになった。さらにコア蛋白＋CYP2E1発現細胞はミトコンドリアGSHの低下を認め，両蛋白の発現がミトコンドリア内での抗酸化作用の低下を助長し，更なる酸化ストレスによりミトコンドリア依存性の細胞死を引き起こすと考えられた。

C型慢性肝疾患患者の病態の特徴のひとつとし

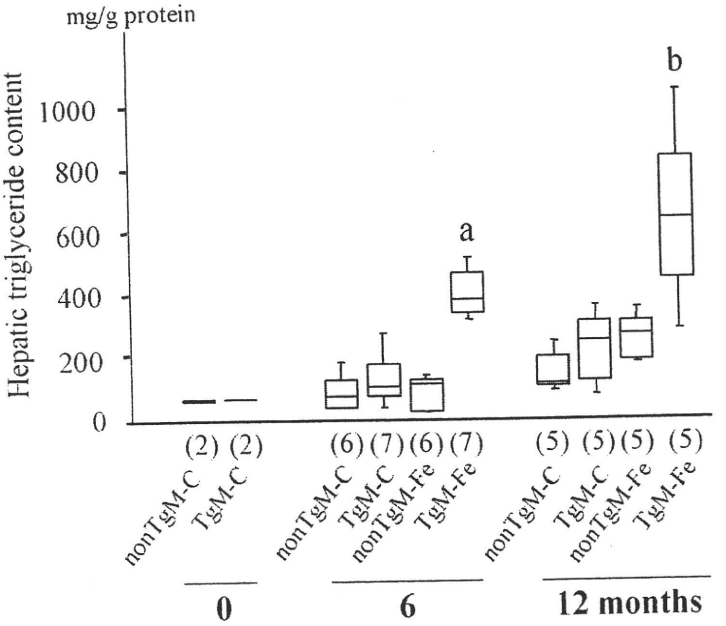

図1
肝内中性脂肪の比較と鉄負荷HCVトランスジェニックマウスの肝組織像（文献7より引用）

nonTgM-C；通常餌飼育コントロールマウス
TgM-C；通常餌飼育トランスジェニックマウス
nonTgM-Fe；鉄過剰餌飼育コントロールマウス
TgM-Fe；鉄過剰餌飼育トランスジェニックマウス
a：P＜.01 vs. 他の3群
b：P＜.01 vs. TgM-C and nonTgM-C，P＜.05 vs. nonTgM-Fe

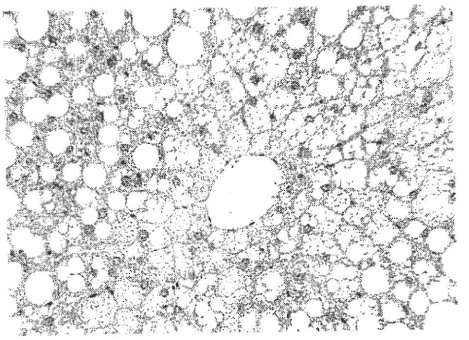

鉄負荷HCVトランスジェニックマウスの肝組織像

て，肝内鉄過剰はよく知られた事実であるが，病態の進展，究極的には肝発癌に及ぼす影響については不明の点も多い。そこで，HCV全遺伝子が組み込まれたトランスジェニックマウス（HCV TgM）を用いて，鉄過剰が肝発癌に及ぼす影響について検討した。まず，HCV TgMと同系のC57BL/6マウス（コントロール）に通常餌あるいは通常餌の5倍量の鉄を含有する餌（鉄過剰餌）を与える4群を設定した。6ヶ月目には鉄過剰餌を与えたHCV TgMは他の3群に比べて有意に肝内の中性脂肪含有量が増加し，組織学的にも中心静脈周囲のmicrovesicular steatosisを混じる脂肪沈着が顕著となり（図1），ミトコンドリアの超微形態にも異常が認められた（図2）。さらにin vivoにおける長鎖脂肪酸の分解能が有意に低下していた。

このように鉄負荷を与えたHCV TgMでは飼育6ヶ月目にしてミトコンドリア異常が明らかとなった。更に12ヶ月目になると鉄負荷HCV TgMでは肝内脂質過酸化物の蓄積が有意に増加し，酸化的DNA傷害の指標である肝内の8-hydroxy-2'-deoxyguanosine (8-OHdG)の含有量が有意に上昇した。最終的には表に示すように鉄負荷HCV TgM群のみに12ヶ月目に11匹中5匹（45%）に肝腫瘍の発生を認め，うち3匹には肝細胞癌が確認された。このようにHCV蛋白の存在に加えて肝内鉄過剰状態が存在するとミトコンドリア障害を介して酸化ストレス，酸化的DNA傷害が惹起され肝発癌に至ることが明らかとなった。

おわりに

HCV蛋白ことにコア蛋白は直接的にミトコンドリア障害を惹起し，酸化ストレスを誘導する。コア蛋白自体による酸化ストレスのmagnitudeはそれほど大きくないものの，HCV蛋白存在下ではアルコールや肝内鉄過剰といった二次的酸化ストレスに対して感受性が亢進しており，相乗的に肝病変が進展することがこれまでの研究から明らかになってきた。抗ウイルス療法によるHCV排除は，酸化ストレスの主要な発生源の消失を意味し最も有効な治療である。

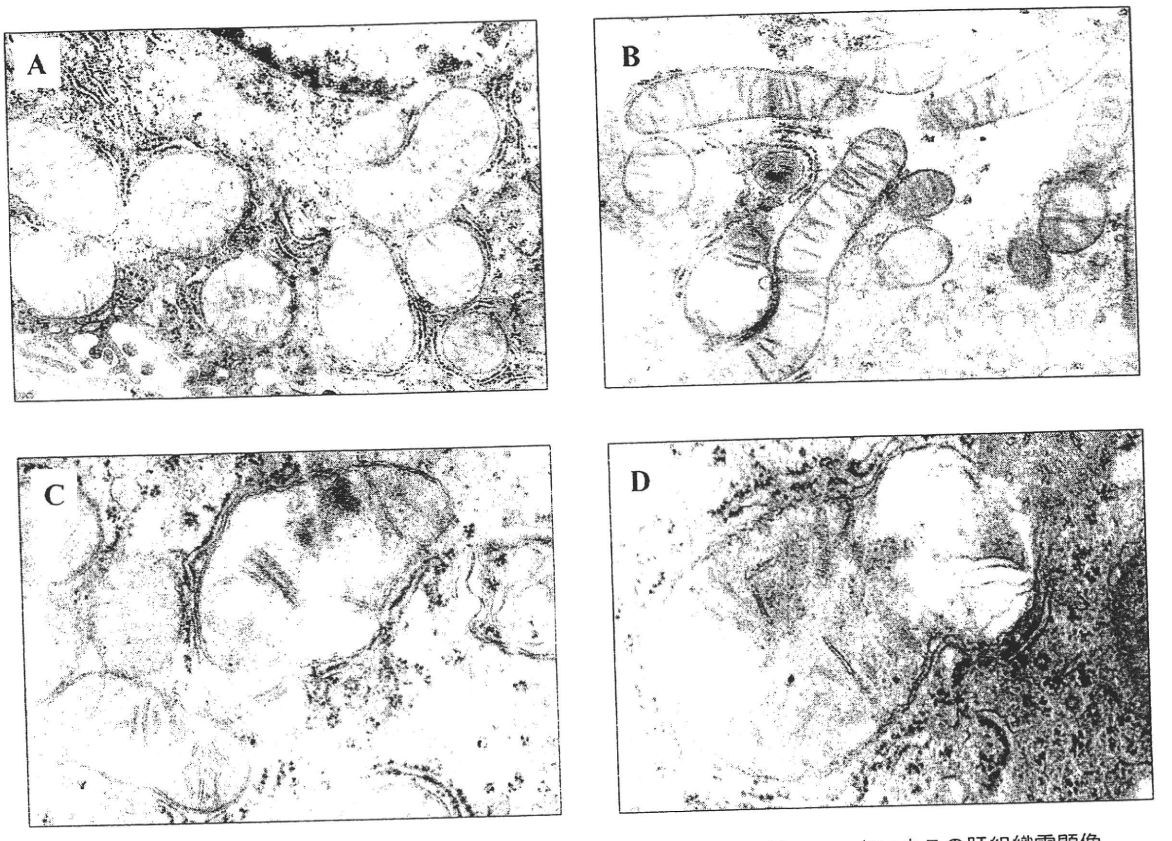

図2　通常餌飼育コントロールマウスと鉄過剰餌飼育HCVトランスジェニックマウスの肝組織電顕像
（文献7より引用）
A：通常餌飼育コントロールマウス
B，C，D：鉄過剰餌飼育HCVトランスジェニックマウス

しかし，その排除率は難治例では50%程度であり，また副作用等で治療を行えない患者も多く存在することから，今後はHCV存在下に酸化ストレスの軽減を目指した治療法が確立されなければならない。

文　献

1) Moriya K, Nakagawa K, Santa T, et al. Cancer Res 2001;11:4365-70.
2) Okuda M, Li K, Beard MR, et al. Gastroenterology 2002;12:366-75.
3) Korenaga M, Wang T, Li Y, et al. J Biol Chem 2005;280:37481-8.
4) Schwer B, Ren S, Pietschmann T, et al. J Virol 2004;78:7958-68.
5) Otani K, Korenaga M, Beard MR, et al. Gastroenterology 2005;128:96-107.
6) Moriya K, Fujie H, Shintani Y, et al. Nat Med 1998;4:1065-7.
7) Furutani T, Hino K, Okuda M, et al. Gastroenterology 2006;130:2087-98.

細胞ニュース

「第79回 日本胃癌学会」

日本胃癌学会は，下記の日程で総会を開催します。

会期：平成19年3月1日（木），2日（金），3日（土）
会場：名古屋国際会議場
会長：山村　義孝（愛知県がんセンター中央病院）
テーマ：胃癌治療　―過去から現在，そして未来へ―
事務局：愛知県がんセンター中央病院　消化器外科
〒464-8681　名古屋市千種区鹿子殿1-1　担当・伊藤
TEL. 052-762-6111

■表紙写真の説明■

肝生検による非アルコール性脂肪性肝炎（NASH）の組織像

脂肪肝を背景にして，小葉中心帯にマロリー体を含んだ肝実質細胞の風船化（ballooning）や細胞浸潤が見られる。

＜表紙写真提供／解説＞　谷川　久一（国際肝臓研究所）

Liver International ISSN 1478-3223

BASIC STUDIES

Stronger Neo-Minophagen C™, a glycyrrhizin-containing preparation, protects liver against carbon tetrachloride-induced oxidative stress in transgenic mice expressing the hepatitis C virus polyprotein

Isao Hidaka[1], Keisuke Hino[2], Masaaki Korenaga[1], Toshikazu Gondo[3], Sohji Nishina[1], Miye Ando[2], Michiari Okuda[1] and Isao Sakaida[1]

1 Department of Gastroenterology and Hepatology, Yamaguchi University Graduate School of Medicine, Ube, Japan
2 Department of Basic Laboratory Sciences, Yamaguchi University Graduate School of Medicine, Ube, Japan
3 Department of Surgical Pathology, Yamaguchi University Hospital, Ube, Japan

Keywords
cytochrome P450 2E1 – γ-glutamylcysteine synthetase – glutathione – mitochondria

Correspondence
Keisuke Hino, MD, PhD, Department of Basic Laboratory Sciences, Yamaguchi University Graduate School of Medicine, 1-1-1 Minami-Kogushi, Ube, Yamaguchi 755-8505, Japan
Tel: +81 836 222 824
Fax: +81 836 222 824
e-mail: k.hino@yamaguchi-u.ac.jp

Received 10 January 2007
accepted 3 March 2007

DOI:10.1111/j.1478-3231.2007.01492.x

Abstract

Background/Aim: Stronger Neo-Minophagen C™ (SNMC), a glycyrrhizin-containing preparation, has been used as a treatment for chronic hepatitis for more than 30 years in Japan, and shown to be effective in preventing the development of hepatocellular carcinoma in chronic hepatitis C patients, but its underlying mechanisms remain elusive. The aim of this study was to investigate if SNMC had an anti-oxidative effect, as oxidative stress has been proposed to be one of the mechanisms of liver injury in hepatitis C virus (HCV)-associated chronic liver diseases. *Methods:* The protective effect of SNMC against carbon tetrachloride (CCl_4)-induced liver injury was examined using transgenic mice expressing the HCV polyprotein. *Results:* A small dose of CCl_4 (10 μl/kg of body weight) significantly increased the serum alanine aminotransferase (ALT) level and hepatic malondialdehyde content, decreased hepatic reduced glutathione (GSH) content and induced ultrastructural alterations of hepatic mitochondria in transgenic mice, but not in nontransgenic mice. A single SNMC treatment equivalent to a clinical dose significantly restored the serum ALT level and hepatic malondialdehyde and GSH contents, attenuated the ultrastructural alterations of hepatic mitochondria, and increased mRNA expression of γ-glutamylcysteine synthetase (γ-GCS). *Conclusions:* Transgenic mice expressing the HCV polyprotein are abnormally vulnerable to oxidative stress. SNMC protects hepatocytes against CCl_4-induced oxidative stress and mitochondrial injury in the presence of HCV proteins by restoring depleted cellular GSH.

Chronic hepatitis C virus (HCV) infection is associated with progressive liver disease that may evolve insidiously to cirrhosis with an increased risk of hepatocellular carcinoma (HCC) and liver failure (1–3). Antiviral treatment with (peg)interferon–ribavirin combination therapy has been successful in 50–85% of patients over the past decade (4, 5). For those not responding or those patients with absolute contraindications to this combination therapy, different treatment strategies are needed. Studies on chronic hepatitis B and C have shown that persistent normalization of alanine aminotransferase (ALT) is important in reducing the complications of chronic hepatitis including development of HCC, regardless of ongoing viral replication (6, 7).

In Japan, a glycyrrhizin-containing preparation, Stronger Neo-Minophagen C™ (SNMC), has been used as a treatment for chronic hepatitis for more than 30 years. It is available in an injectable form for intravenous administration, containing 0.2% glycyrrhizin, 0.1% L-cystein and 2.0% glycine in physiologic solution. Glycyrrhizin is an aqueous extract of licorice root (*Glycyrrhizae radix*), which has anti-allergic, anti-inflammatory and detoxicating effects (8). The anti-

inflammatory mechanism of SNMC is thought to be owing to its protective effect on the hepatic cellular membrane (9, 10). In a double-blind randomized placebo-controlled trial, Suzuki et al. (11) reported that in Japanese patients with chronic hepatitis, serum transaminases decreased during the treatment with SNMC. A recent European randomized trial also showed biochemical and histological effects of 26-week treatment with SNMC in patients with chronic hepatitis C (12). In addition, Arase et al. (13) demonstrated that long-term usage of SNMC was effective in preventing HCC development in Japanese patients with chronic hepatitis C. However, that study was retrospective and the mechanisms by which SNMC prevents HCC development remain elusive.

Oxidative stress has been proposed to be one of the mechanisms of liver injury in HCV-associated chronic liver diseases (14–17) and increased markers of oxidative stress are a well-known feature (18–20). Oxidative stress favours DNA damage, genetic instability and tumorigenesis. Indeed, we have reported that HCV transgenic mice fed an excess iron diet show marked steatosis and mitochondrial injury at 6 months, and an increase in the hepatic content of lipid peroxidation products and 8-hydroxy-2′-deoxyguanosine and subsequent development of HCC at 12 months after the initiation of feeding (21). This animal model, therefore, seemed to be useful for studying the mechanisms by which the long-term treatment with SNMC prevents HCC development in persistent HCV infection. In addition, we chose to use carbon tetrachloride (CCl_4) to induce mild oxidative stress in transgenic mice, since we previously observed that a low dose of CCl_4 caused the liver damage with oxidative stress in other HCV transgenic mice (16). The aim of this study was to ascertain if SNMC had a protective effect against the liver damage with oxidative stress, which would provide us with a rationale for conducting long-term treatment with SNMC in HCV transgenic mice.

Materials and methods

Animals

The transgene pAlbSVPA-HCV, containing the full-length polyprotein-coding region (core to NS5B, nts 342-9378) of genotype 1b, of the HCV-N strain of HCV (22), under the control of the murine albumin promoter/enhancer, was described in detail by Lerat et al. (23). Of the four transgenic lineages with evidence of ribonucleic acid (RNA) transcription of the full-length HCV-N open reading frame (FL-N), the FL-N/35 lineage proved capable of breeding in large numbers. There was no inflammation in transgenic livers (23). Transgenic animals were mated with normal C57BL/6 mice to produce subsequent-generation animals. These subsequent-generation animals were identified by polymerase chain reaction (PCR) analysis, as described previously (21). FL-N/35 transgenic mice and age-matched C57BL/6 mice were bred and maintained according to the criteria outlined in the 'Guide for the Care and Use of Laboratory Animals'.

Experimental design

FL-N/35 transgenic male mice and their normal C57BL/6 male littermates (nontransgenic mice) aged 3 months were injected intraperitoneally with 10 μl/kg of body weight CCl_4 (Wako Pure Chemical, Osaka, Japan) in corn oil with/without subsequent subcutaneous injection of 50 μl of SNMC (supplied by Minophagen Pharmaceutical Co. Ltd, Tokyo, Japan) 30 min after CCl_4 injection: nontransgenic mice were injected with CCl_4, FL-N/35 transgenic mice with CCl_4, nontransgenic mice with CCl_4 followed by SNMC and FL-N/35 transgenic mice with CCl_4 followed by SNMC. SNMC consists of 40 mg of glycyrrhizin, 20 mg L-cystein and 400 mg of glycine in 20 ml of physiological saline. Untreated animals were used as controls. Four to six mice in each group were killed by intraperitoneal injection of 10% pentobarbital sodium at 12 or 24 h after CCl_4 injection, and blood samples and liver tissue were collected for determination of the serum ALT level, hepatic content of lipid peroxidation products, cytochrome P450 2E1 (CYP2E1), reduced glutathione (GSH) and γ-glutamylcysteine synthetase (γ-GCS) and histology.

Hepatic lipid peroxidation-derived adducts

Resected fresh liver tissues were weighed and homogenized with saline. Homogenates were assayed for lipid peroxidation products. Malondialdehyde (MDA), one of aldehydic metabolites of lipid peroxidation, was quantified by the method of Yagi (24), by using a WAKO lipid peroxidation-test (Wako Pure Chemical). Hepatic MDA content was expressed as nanomoles per gram of liver weight.

Histological procedures

A portion of liver tissue was immediately snap frozen in liquid nitrogen for RNA extraction, protein extraction and determination of the hepatic GSH level. The remaining liver tissue was fixed in 4% paraformaldehyde in phosphate-buffered saline and embedded in paraffin for histological analysis. Liver sections were

stained with H&E and Masson's trichrome method for fibrosis.

Electron microscopy

Liver specimens were fixed in 2.1% glutaraldehyde, postfixed in 1% osmium tetroxide, dehydrated in graded ethanol and propylene dioxide, and embedded in Epok. Thin sections were stained with uranyl acetate and lead citrate and examined using a Hitachi-7000 transmission electron microscope (Hitachi Ltd, Tokyo, Japan).

Immunoblotting of cytochrome P450 2E1 (CYP2E1)

Resected liver tissues were homogenized in cell lysis buffer (Daiichi-Kagaku, Tokyo, Japan), containing 10 μl/ml of protease inhibitor cocktail (Sigma, St Louis, MO, USA) and 1 mM phenylmethylsulphonyl fluoride (Roche Molecular Biochemicals, Tokyo, Japan). Protein samples (20 μg of protein) were separated by sodium dodecyl sulphate-polyacrylamide gel electrophoresis on a 10–20% gel. The proteins were electrophoretically transferred to polyvinylidene difluoride membranes (Millipore, Bedford, MA, USA), blocked overnight at 4 °C with 5% skimmed milk and 0.1% Tween 20 in Tris-buffered saline and subsequently incubated for 1 h at room temperature with a goat polyclonal anti-rat CYP2E1 antibody (1:3000; Daiichi-Kagaku, Tokyo, Japan). This anti-rat antibody has been shown to work in mice (25). The membranes were washed, incubated with appropriate secondary antibodies and detected with ECLTM Western blot detection reagents (Amersham Biosciences, Piscataway, NJ, USA).

Hepatic content of GSH

Fifty milligrams of liver tissues was minced and sonicated in ice-cold 5% trichloroacetic acid and centrifuged at 3000g at 4 °C for 10 min. GSH content in the liver was measured by the thioester method, using a GSH-400 kit (OXIS International Inc., Portland, OR, USA). Protein concentrations in liver were determined by the method of Bradford et al. (26), by using the Quick start Bradford™ Dye Reagent (Bio-Rad Laboratories Inc., Hercules, CA, USA). Hepatic GSH content was expressed as nanomole per milligram of protein in the liver.

Messenger RNA expression (mRNA) of γ-glutamylcysteine synthetase (γ-GCS)

Total RNA was extracted from the frozen liver tissues using an RNeasy mini kit (Qiagen, Hilden, Germany). One-step real-time reverse transcription (RT)-PCR was performed with a Light Cycler using a QuantiTect SYBR Green RT-PCR Kit (Qiagen), according to the manufacturer's instructions. The melting-point analysis of all samples and controls was performed within the range from 65 to 95 °C. The primers amplifying the genes coding the heavy subunit (γ-GCS_H) and light subunit (γ-GCS_L) of γ-GCS are described in Table 1. The relative quantities of target mRNA used in the real-time RT-PCR were normalized with β-actin to compensate for variations in input RNA amounts.

Statistical analysis

Quantitative values are expressed as mean ± standard deviation. Two groups among multiple groups were compared by the rank-based, Kruskal–Wallis analysis of variance test followed by Scheffe's test because of non-homogeneity of variance among the groups. Data between two different groups were compared by the Mann–Whitney test. A P value of < 0.05 was considered to be significant.

Results

CCl_4-induced oxidative stress in FL-N/35 transgenic mice

Serum ALT levels remained normal in the basal condition in FL-N/35 transgenic and nontransgenic mice. FL-N/35 transgenic mice had significantly higher ALT levels in serum ($P < 0.0001$) at 24 h after intraperitoneal injection of CCl_4 as compared with those of the basal condition, but nontransgenic mice did not (Fig.

Table 1. Primers of the genes coding the heavy subunit (γ-GCS_H) and light subunit (γ-GCS_L) of γ-GCS

Genes	Sense	Antisense
γ-GCS_H	CTCCAGGTGACATTCCAAGCC[1]	GGCAGAAATCACTCCCCAGC[1]
γ-GCS_L	CACAATGACCCGAAAGAACTGCT[2]	GACTTGATGATTCCCCTGCTCTTC[2]
β-actin	TGACAGGATGCAGAAGGAGA[3]	GCTGGAAGGTGGACAGTGAG[3]

GenBank accession numbers are NM_010295 for 1, NM_008129 for 2, and NM_007393 for 3.
γ-GCS, γ-glutamylcysteine synthetase.

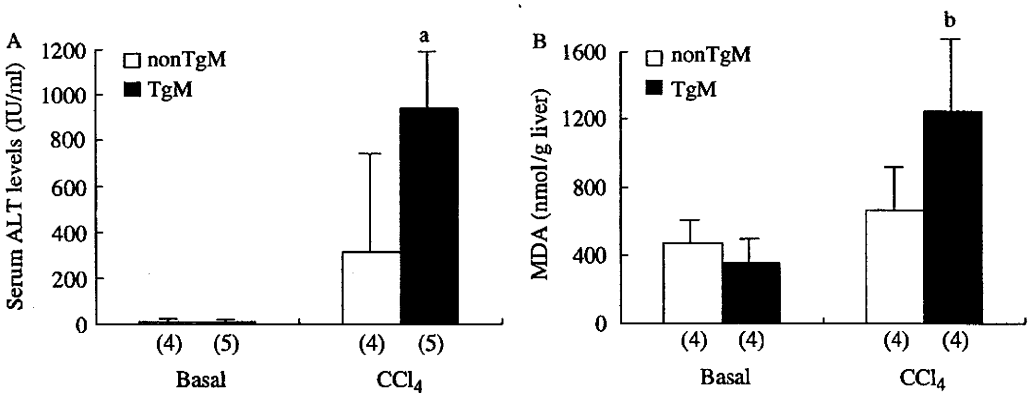

Fig. 1. Serum alanine aminotransferase (ALT) levels (A) and hepatic malondialdehyde (MDA) content (B) in FL-N/35 transgenic and nontransgenic mice in basal and carbon tetrachloride (CCl_4)-injected conditions. The numbers in parentheses represent the number of animals examined in each group. TgM, FL-N/35 transgenic mice; nonTgM, nontransgenic mice; a, $P < 0.0001$ vs TgM in basal condition; b, $P < 0.005$ vs TgM in basal condition.

1A). Similarly, there was no difference in hepatic MDA levels between FL-N/35 transgenic and nontransgenic mice in the basal condition. Intraperitoneal injection of CCl_4 significantly increased hepatic MDA levels after 24 h in FL-N/35 transgenic mice ($P = 0.005$), but not in nontransgenic mice (Fig. 1B). Nontransgenic mice did not show any significant histological changes such as inflammatory cell infiltration or hepatocytic degeneration at 24 h after CCl_4 injection. Liver histology of FL-N/35 transgenic mice after CCl_4 injection showed no infiltration of inflammatory cells, but swelling of hepatocytes in the perivenular zone (zone III) and mild steatosis, including the microvesicular type in the perivenular region and mid-zone (zone II) (Fig. 2A–D). The swollen hepatocytes seemed to contain vacuoles when observed at × 400 magnification. Thus, the small dose of CCl_4 used in the present study caused oxidative stress in FL-N/35 transgenic mice, but not in nontransgenic mice, which implied that FL-N/35 transgenic mice were more sensitive to oxidative stress than nontransgenic mice.

Protective effect of SNMC against CCl_4-induced oxidative stress in FL-N/35 transgenic mice

The CCl_4-induced significant increase in serum ALT levels was almost completely reversed by subcutaneous injection of 50 µl of SNMC 30 min after CCl_4 treatment in FL-N/35 transgenic mice ($P = 0.0009$) (Fig. 3A). SNMC treatment also restored the CCl_4-induced significantly increased MDA level in the liver to the basal level or reduced below it in FL-N/35 transgenic mice ($P = 0.0006$) (Fig. 3B). We next examined the hepatic content of GSH in FL-N/35 transgenic mice, since SNMC improved the liver injury induced by CCl_4. Although serum ALT levels and hepatic MDA levels significantly increased at 24 h after intraperitoneal injection of CCl_4, hepatic content of GSH was comparable with the basal level at this time point. However, the hepatic content of GSH significantly decreased at 12 h after CCl_4 injection in FL-N/35 transgenic mice as compared with the basal level ($P < 0.05$) (Fig. 3C). These results suggested that the hepatic GSH level was potentially restored by 24 h after CCl_4 administration. The depleted hepatic GSH content at 12 h after CCl_4 injection was restored by the treatment with SNMC in FL-N/35 transgenic mice ($P = 0.005$) (Fig. 3C). The swollen hepatocytes were absent and steatosis was less frequent in the liver in FL-N/35 transgenic mice treated with SNMC after CCl_4 injection (Fig. 2C–F). Thus, SNMC improved the liver injury induced by CCl_4 in FL-N/35 transgenic mice.

Hepatic expression of CYP2E1

Metabolism of CCl_4 begins with the formation of the trichloromethyl free radicals through the action of the cytochrome P450 oxygenase system of the endoplasmic reticulum (27). The major cytochrome isozyme that executes biotransformation of CCl_4 is CYP2E1. We therefore examined the hepatic expression of CYP2E1 in FL-N/35 transgenic mice on the assumption that SNMC may prevent the CCl_4-induced increase in CYP2E1 expression. However, CCl_4 injection did not increase the hepatic expression of CYP2E1 nor did SNMC change the hepatic expression of CYP2E1 at 12 and 24 h after CCl_4 injection (Fig. 4).

Ultrastructural alterations of mitochondria

As treatment with SNMC attenuated the CCl_4-induced swelling of hepatocytes and steatosis including

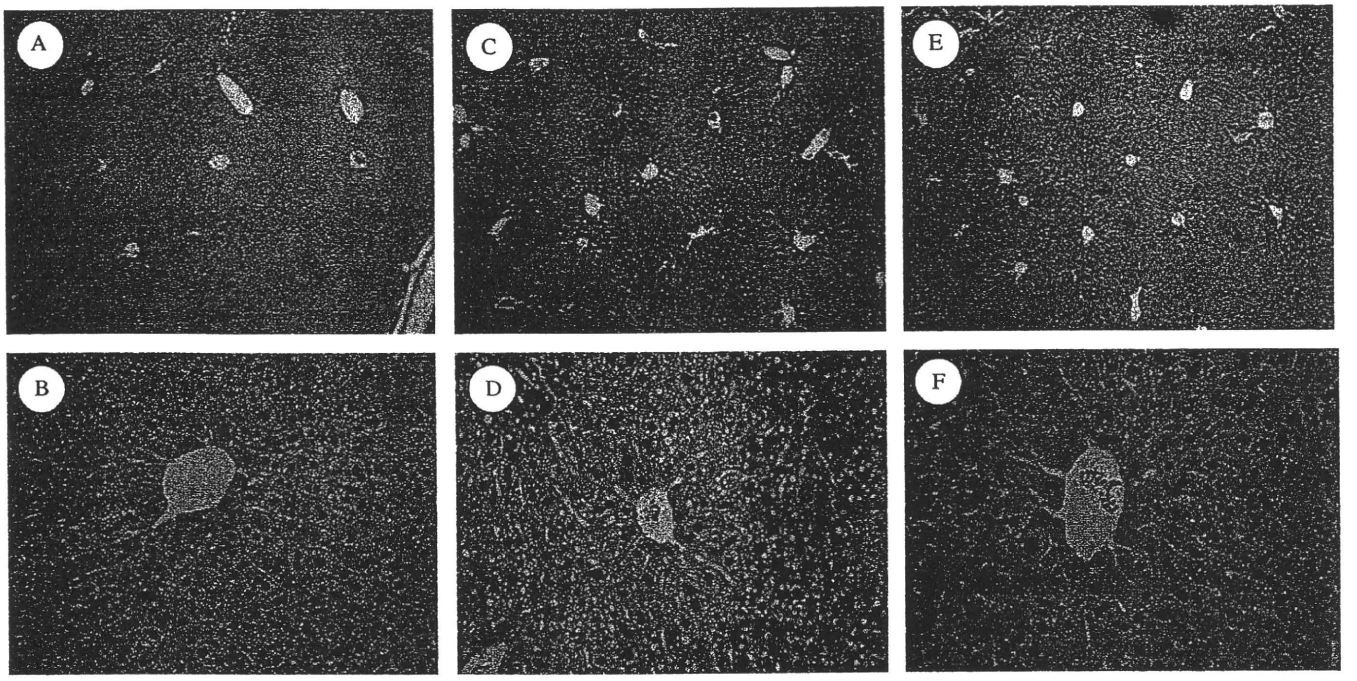

Fig. 2. Liver histology of FL-N/35 transgenic mice in basal (A and B) and carbon tetrachloride (CCl_4)- (C and D) or CCl_4 plus Stronger Neo-Minophagen C^{TM} (SNMC)-injected conditions (E and F) (H&E, original magnification × 100 for A, C and E, × 400 for B, D and F). Liver histology of FL-N/35 transgenic mice after CCl_4 injection shows swelling of hepatocytes in the perivenular zone and mild steatosis including the microvesicular type, in the perivenular region and midzone. Such hepatocytic swelling was absent and steatosis was less frequent in the liver in FL-N/35 transgenic mice treated with SNMC after CCl_4 injection.

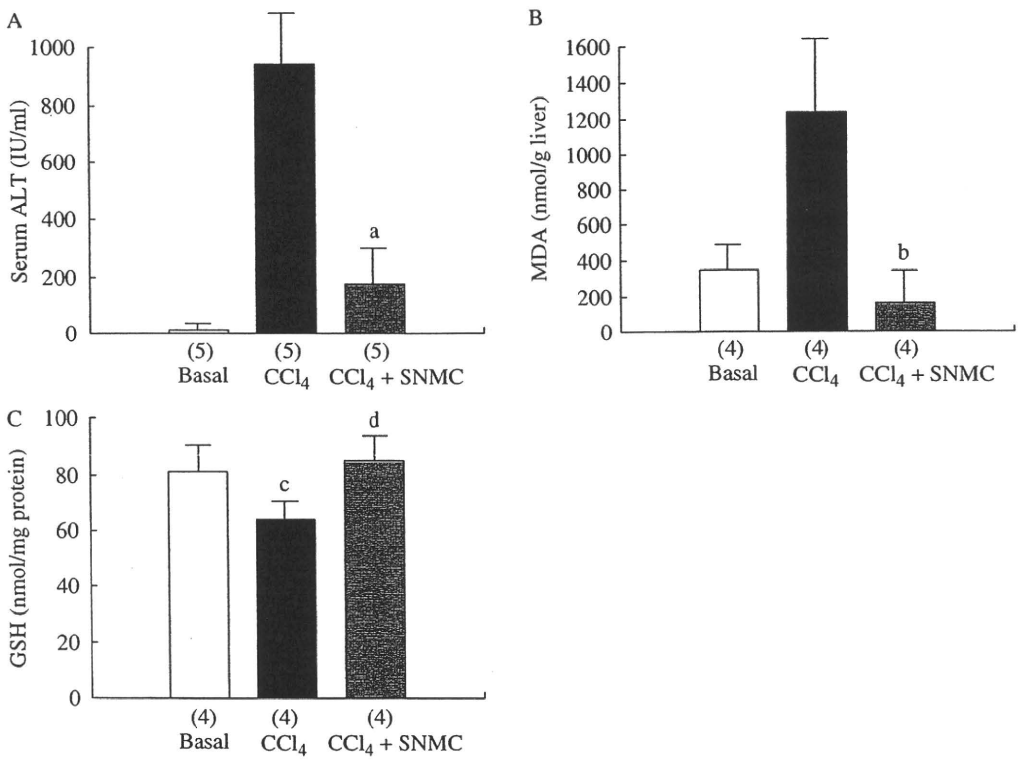

Fig. 3. Serum alanine aminotransferase (ALT) levels (A), hepatic malondialdehyde (MDA) content (B) and hepatic glutathione (GSH) content (C) in FL-N/35 transgenic mice in basal, carbon tetrachloride (CCl_4)- or CCl_4 plus Stronger Neo-Minophagen C^{TM} (SNMC)-injected conditions. The numbers in parentheses represent the number of animals examined in each group. a, $P = 0.0009$ vs mice with CCl_4; b, $P = 0.0006$ vs mice with CCl_4; c, $P = .01$ vs mice in the basal condition; d, $P = 0.005$ vs mice with CCl_4.

the microvesicular type, we next examined the ultrastructure of the hepatocytic mitochondria in FL-N/35 transgenic mice. Even a modest dose of CCl_4 caused swelling of mitochondria in FL-N/35 transgenic mice. Such swollen mitochondria or irregular-sized mitochondria were less frequently found in FL-N/35 transgenic mice treated with SNMC after CCl_4 injection than in those without SNMC treatment (Fig. 5). Thus, SNMC attenuated the ultrastructural alterations of mitochondria induced by CCl_4 injection in FL-N/35 transgenic mice, suggesting that SNMC potentially protects mitochondria against oxidative stress.

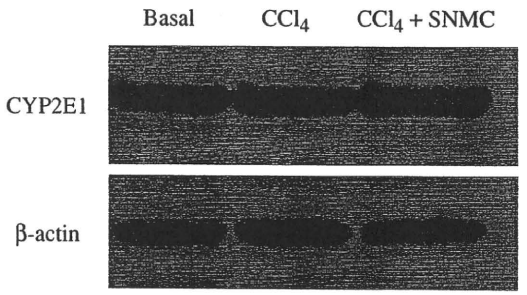

Fig. 4. Hepatic expression of CYP2E1 in FL-N/35 transgenic mice at 12 h after carbon tetrachloride (CCl_4) injection. Immunoblots for CYP2E1 were performed on liver lysates obtained from four mice in each group at 12 and 24 h after CCl_4 injection. CCl_4 injection did not increase the hepatic expression of CYP2E1 nor did Stronger Neo-Minophagen C™ (SNMC) change the hepatic expression of CYP2E1 at both time points.

mRNA expression of γ-GCS

γ-GCS is a heterodimer composed of γ-GCS_H and γ-GCS_L that associates, through disulphide binding, to form the holoenzyme (28, 29). We examined the mRNA expression of both subunits of γ-GCS at 12 h after CCl_4 injection in FL-N/35 transgenic mice, since SNMC-induced recovery from depletion of hepatic GSH was found at this time. In parallel with GSH, the expression of γ-GCS_L was significantly increased by the treatment with SNMC after CCl_4 injection ($P < 0.05$) (Fig. 6).

Discussion

Oxidative stress has been proposed to be one of the mechanisms of liver injury in HCV-associated chronic liver diseases (14–17) and increased markers of oxidative stress are a well-known feature in them (18–20).

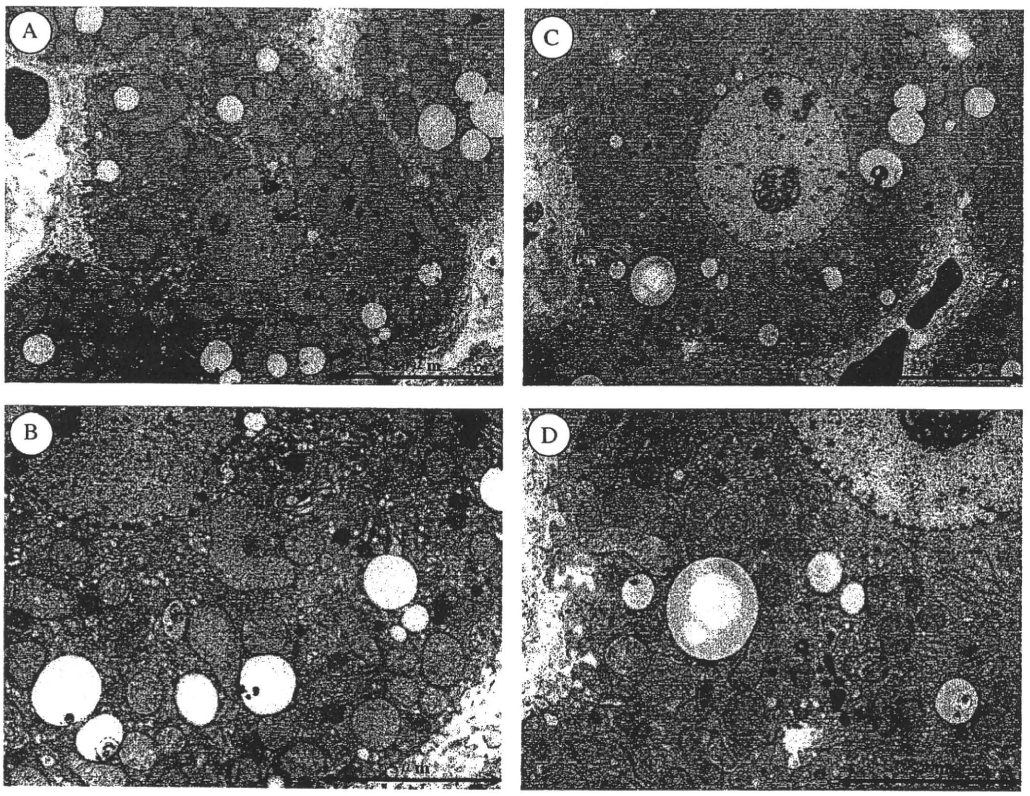

Fig. 5. Electron microscopy of the livers of FL-N/35 transgenic mice after carbon tetrachloride (CCl_4) injection (A and B) and CCl_4 plus Stronger Neo-Minophagen C™ (SNMC) injection (C and D). Swollen or irregular-sized mitochondria were less frequently found in FL-N/35 transgenic mice treated with SNMC after CCl_4 injection than in those without SNMC treatment (original magnification × 2000 for A and C, × 5000 for B and D).

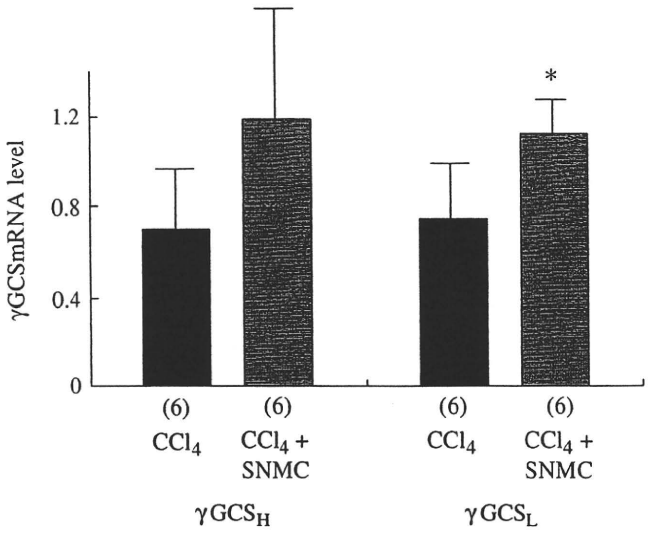

Fig. 6. Hepatic γ-glutamylcysteine synthetase (γ-GCS) mRNA levels in FL-N/35 transgenic mice at 12 h after injection of carbon tetrachloride (CCl_4) alone or CCl_4 plus Stronger Neo-Minophagen C™ (SNMC). The numbers in parentheses represent the number of animals examined in each group. $^*P < 0.05$ vs mice with CCl_4.

However, the magnitude of oxidative stress induced by HCV proteins itself may not be large, as shown by the slow progression of liver disease in chronic hepatitis C patients with persistently normal aminotransferase levels. Clinical factors such as alcohol, iron overload and/or aging have been shown to reinforce the progression of liver disease in HCV infection (30–32). Oxidative stress induced by combination of HCV proteins with those factors is assumed to favour DNA damage, genetic instability and tumorigenesis. Long-term treatment with SNMC has been shown to be effective in preventing the development of HCC in patients with chronic hepatitis C (13). In this context, we wanted to know if SNMC had a protective effect against oxidative stress induced by the combination of HCV proteins with secondary stimulation, and examined this using transgenic mice expressing the HCV polyprotein. We chose to use CCl_4 to induce mild oxidative stress in transgenic mice. The type and extent of liver injury induced by CCl_4 cover a wide range of effects, depending on the dose and duration of exposure, or time of observation (33). The dose (10 μl/kg body weight) of CCl_4 used in this study was much less than those used for inducing oxidative stress in mice in previous studies (34–36), as we aimed to induce mild oxidative stress that was comparable with the clinical one observed in patients with chronic hepatitis C. This may explain why the expression of CYP2E1 was not significantly increased after CCl_4 treatment in FL-N/35 transgenic mice, even though CYP2E1 plays a central role in metabolizing CCl_4 (33). It should be noted that even such a small dose of CCl_4 induced a significant increase in serum ALT and hepatic MDA levels, and histological changes in FL-N/35 transgenic mice, though not in nontransgenic mice. These results show that FL-N/35 transgenic mice are abnormally vulnerable to oxidative stress. This observation is consistent with our previous observation that oxidative stress was significantly intensified by modest iron supplementation in FL-N/35 transgenic mice, but not in nontransgenic mice (21). Mitochondria are one of the main subcellular structures of hepatocytes affected by CCl_4 exposure (33). Even modest CCl_4 administration, which did not increase the expression of CYP2E1, caused ultrastructural alterations of hepatocytic mitochondria in FL-N/35 transgenic mice. In this context mitochondrial electron transport has been shown to be responsible for the free-radical activation by CCl_4 without the influence of CYP2E1 (37). We also reported that HCV core protein inhibits mitochondrial electron transport and increases reactive oxygen species production (17). Therefore, the small dose of CCl_4 may have reinforced the mitochondrial injury induced by HCV proteins. This may in part explain why FL-N/35 transgenic mice are abnormally vulnerable to oxidative stress. Thus, the CCl_4-induced mild oxidative stress observed in FL-N/35 transgenic mice seemed to be suitable for mimicking the oxidative stress induced by combination of HCV proteins with clinical factors such as alcohol, iron overload or aging in patients with HCV-associated chronic liver diseases.

The dose of SNMC administered to the FL-N/35 transgenic mice was comparable with the dosage given to patients with chronic hepatitis (approximately 100 ml of SNMC). This implies that a clinical dosage of SNMC is enough to reduce oxidative stress occurring in patients with HCV-associated chronic liver diseases. It should also be noted that SNMC treatment using a dose equivalent to a clinical dosage attenuated ultrastructural alterations of mitochondria induced by CCl_4. We previously reported the development of HCC preceded by marked hepatic steatosis, ultrastructural alterations of the mitochondria, decreased degradation activity of fatty acid and increases in the hepatic content of lipid peroxidation products in FL-N/35 transgenic mice fed an excess iron diet (21). In fact, we found that hepatic triglyceride content was significantly decreased by a 6-month treatment with SNMC in FL-N/35 transgenic mice fed the excess iron diet (I. Hidaka et al., unpublished observations). Therefore, SNMC appears to have the potential to prevent HCC development by reducing mitochondrial

injury induced by HCV and additional oxidative stress. Trichloromethyl free radicals derived from CCl_4 react with sulphthydyl groups such as GSH and protein thiols, and the covalent binding of trichloromethyl free radicals to the cell membrane is considered the initial step in a chain of events that eventually leads to membrane lipid peroxidation and finally to cell necrosis. It remains elusive whether GSH was primarily consumed against cytoplasmic oxidative tress or against mitochondrial oxidative stress or against both in the present model. Judging from the protective effect of SNMC against mitochondrial injury induced by CCl_4, inhibition of GSH depletion by SNMC may have contributed to reduction in mitochondrial oxidative stress in FL-N/35 transgenic mice. Hepatic GSH synthesis is mainly regulated by the availability of cysteine, the sulphur amino acid precursor, and the activity of the rate-limiting enzyme γ-GCS (38). SNMC consists of 0.2% glycyrrhizin, 0.1% cysteine and 2.0% glycine in physiologic solution. Originally SNMC was developed with the expectation of joint beneficial effects of the three components. The cysteine included in SNMC may have contributed to GSH synthesis through its increased availability. SNMC treatment also increased the synthesis of γ-GCS_L at the transcriptional level ($P < 0.05$). There are at least three possibilities that may account for this. First, glycyrrhizin may have activated γ-GCS at the transcriptional level. Second, cysteine may have activated γ-GCS as a substrate for γ-GCS. Third, both of the above may have worked together. The increase in γ-GCS_H expression by SNMC may have failed to reach a statistical significance ($P = 0.08$) owing to its greater deviation.

In conclusion, this study shows that transgenic mice expressing the HCV polyprotein are abnormally vulnerable to oxidative stress and that SNMC protects hepatocytes against CCl_4-induced oxidative stress in the presence of HCV proteins. SNMC also has protective effect against mitochondrial injury induced by CCl_4 in HCV transgenic mice.

References

1. Di Bisceglie AM, Goodman ZD, Ishak KG, Hoofnagle JH, Melpolder JJ, Alter HJ. Long-term clinical and histopathological follow-up of chronic posttransfusion hepatitis. *Hepatology* 1991; **14**: 969–74.
2. Tsukuma H, Hiyama T, Tanaka S, *et al.* Risk factors for hepatocellular carcinoma among patients with chronic liver disease. *N Engl J Med* 1993; **328**: 1797–801.
3. Tong MJ, el-Farra NS, Reikes AR, Co RL. Clinical outcomes after transfusion-associated hepatitis C. *N Engl J Med* 1995; **332**: 1463–6.
4. Manns MP, McHutchison JG, Gordon SC, *et al.* Peginterferon alfa-2b plus ribavirin compared with interferon alfa-2b plus ribavirin for initial treatment of chronic hepatitis C: a randomised trial. *Lancet* 2001; **358**: 958–65.
5. Fried MW, Shiffman ML, Reddy KR, *et al.* Peginterferon alfa-2a plus ribavirin for chronic hepatitis C virus infection. *N Engl J Med* 2002; **347**: 975–82.
6. Fattovich G, Giustina G, Degos F, *et al.* Effectiveness of interferon alfa on incidence of hepatocellular carcinoma and decompensation in cirrhosis type C. European concerted action on viral heaptitis (EUROHEP). *J Hepatol* 1997; **27**: 201–5.
7. Kasahara A, Hayashi N, Mochizuki K, *et al.* Risk factors for hepatocellular carcinoma and its incidence after interferon treatment in patients with chronic hepatitis C. Osaka liver disease study group. *Hepatology* 1998; **27**: 1394–402.
8. Finney RSH, Somers GF. The anti-inflammatory activity of glycyrrhetinic acid and derivatives. *J Pharm Pharmacol* 1958; **10**: 613–20.
9. Nakamura T, Fujii T, Ichihara A. Enzyme leakage due to change of membrane permeability of primary cultured rat hepatocytes treated with various hepatotoxins and its prevention by glycyrrhizin. *Cell Biol Toxicol* 1985; **1**: 285–95.
10. Shiki Y, Shirai K, Saito Y, Yoshida S, Mori Y, Wakashin M. Effect of glycyrrhizin on lysis of hepatocyte membranes induced by anti-liver cell membrane antibody. *J Gastroenterol Hepatol* 1992; **7**: 12–6.
11. Suzuki H, Ohta Y, Takino T, Fujisawa K, Hirayama C. Effects of glycyrrhizin on biochemical tests in patients with chronic hepatitis. *Asian Med J* 1983; **26**: 423–38.
12. Orlent H, Hansen BE, Willems M, *et al.* Biochemical and histological effects of 26 weeks of glycyrrhizin treatment in chronic hepatitis C: a randomized phase II trial. *J Hepatol* 2006; **45**: 539–46.
13. Arase Y, Ikeda K, Murashima N, *et al.* The long term efficacy of glycyrrhizin in chronic hepatitis C patients. *Cancer* 1997; **79**: 1494–500.
14. Barbaro G, Di Lorenzo G, Asti A, *et al.* Hepatocellular mitochondrial alterations in patients with chronic hepatitis C: ultrastructural and biochemical findings. *Am J Gastroenterol* 1999; **94**: 2198–205.
15. Valgimigli M, Valgimigli L, Trere D, *et al.* Oxidative stress EPR measurement in human liver by radical-probe technique. Correlation with etiology, histology and cell proliferation. *Free Radic Res* 2002; **36**: 939–48.
16. Okuda M, Li K, Beard MR, *et al.* Mitochondrial injury, oxidative stress, and antioxidant gene expression are induced by hepatitis C virus core protein. *Gastroenterology* 2002; **122**: 366–75.
17. Korenaga M, Wang T, Li Y, *et al.* Hepatitis C virus core protein inhibits mitochondrial electron transport and increases

reactive oxygen species (ROS) production. *J Biol Chem* 2005; **280**: 37481–8.
18. Jain SK, Pemberton PW, Smith A, *et al.* Oxidative stress in chronic hepatitis C: not just a feature of late stage disease. *J Hepatol* 2002; **36**: 805–11.
19. Paradis V, Mathurin P, Kollinger M, *et al.* In situ detection of lipid peroxidation in chronic hepatitis C: correlation with pathological features. *J Clin Pathol* 1997; **50**: 401–6.
20. Kitase A, Hino K, Furutani T, *et al.* In situ detection of oxidized n-3 polyunsaturated fatty acids in chronic hepatitis C: correlation with hepatic steatosis. *J Gastroenterol* 2005; **40**: 617–24.
21. Furutani T, Hino K, Okuda M, *et al.* Hepatic iron overload induces hepatocellular carcinoma in transgenic mice expressing the hepatitis C virus polyprotein. *Gastroenterology* 2006; **130**: 2087–98.
22. Beard MR, Abell G, Honda M, *et al.* An infectious molecular clone of a Japanese genotype 1b hepatitis C virus. *Hepatology* 1999; **30**: 316–24.
23. Lerat H, Honda M, Beard MR, *et al.* Steatosis and liver cancer in transgenic mice expressing the structural and nonstructural proteins of hepatitis C virus. *Gastroenterology* 2002; **122**: 352–65.
24. Yagi K. A simple fluorometric assay for lipoperoxide in blood plasma. *Biochem Med* 1976; **15**: 212–6.
25. Healy LN, Pluta LJ, Recio L. Expression and distribution of cytochrome P450 2E1 in B6C3F1 mouse liver and testes. *Chem Biol Interact* 1999; **121**: 199–207.
26. Bradford MM. A rapid and sensitive method for the quantitation of microgram quantities of protein utilizing the principle of protein-dye binding. *Anal Biochem* 1976; **72**: 248–54.
27. Recknagel RO, Glende EA Jr, Dolak JA, Waller RL. Mechanisms of carbon tetrachloride toxicity. *Pharmacol Ther* 1989; **43**: 139–54.
28. Yan N, Meister A. Amino acid sequence of rat kidney gamma-glutamylcysteine synthetase. *J Biol Chem* 1990; **265**: 1588–93.
29. Gipp JJ, Bailey HH, Mulcahy RT. Cloning and sequencing of the cdna for the light subunit of human liver gamma-glutamylcysteine synthetase and relative mrna levels for heavy and light subunits in human normal tissues. *Biochem Biophys Res Commun* 1995; **206**: 584–9.
30. Poynard T, Bedossa P, Opolon P. Natural history of liver fibrosis progression in patients with chronic hepatitis C. The OBSVIRC, METAVIR, CLINIVIR, and DOSVIRC goups. *Lancet* 1997; **349**: 825–32.
31. Kato J, Kobune M, Nakamura T, *et al.* Normalization of elevated hepatic 8-hydroxy-2′-deoxyguanosine levels in chronic hepatitis C patients by phlebotomy and low iron diet. *Cancer Res* 2001; **61**: 8697–702.
32. Murakami C, Hino K, Korenaga M, *et al.* Factors predicting progression to cirrhosis and hepatocellular carcinoma in patients with transfusion-associated hepatitis C virus infection. *J Clin Gastroenterol* 1999; **28**: 148–52.
33. Weber LW, Boll M, Stampfl A. Hepatotoxicity and mechanism of action of haloalkanes: carbon tetrachloride as a toxicological model. *Crit Rev Toxicol* 2003; **33**: 105–36.
34. Jeong HG, You HJ, Park SJ, *et al.* Hepatoprotective effects of 18beta-glycyrrhetinic acid on carbon tetrachloride-induced liver injury: inhibition of cytochrome P450 2E1 expression. *Pharmacol Res* 2002; **46**: 221–7.
35. Wang L, Potter JJ, Rennie-Tankersley L, Novitskiy G, Sipes J, Mezey E. Effects of retinoic acid on the development of liver fibrosis produced by carbon tetrachloride in mice. *Biochim Biophys Acta* 2007; **1772**: 66–71.
36. Lopez-Diazguerrero NE, Luna-Lopez A, Gutierrez-Ruiz MC, Zentella A, Konigsberg M. Susceptibility of DNA to oxidative stressors in young and aging mice. *Life Sci* 2005; **77**: 2840–54.
37. Tomasi A, Albano E, Banni S, *et al.* Free-radical metabolism of carbon tetrachloride in rat liver mitochondria. A study of the mechanism of activaion. *Biochem J* 1987; **246**: 313–7.
38. Lu SC. Regulation of hepatic glutathione synthesis: current concepts and controversies. *FASEB J* 1999; **13**: 1169–83.

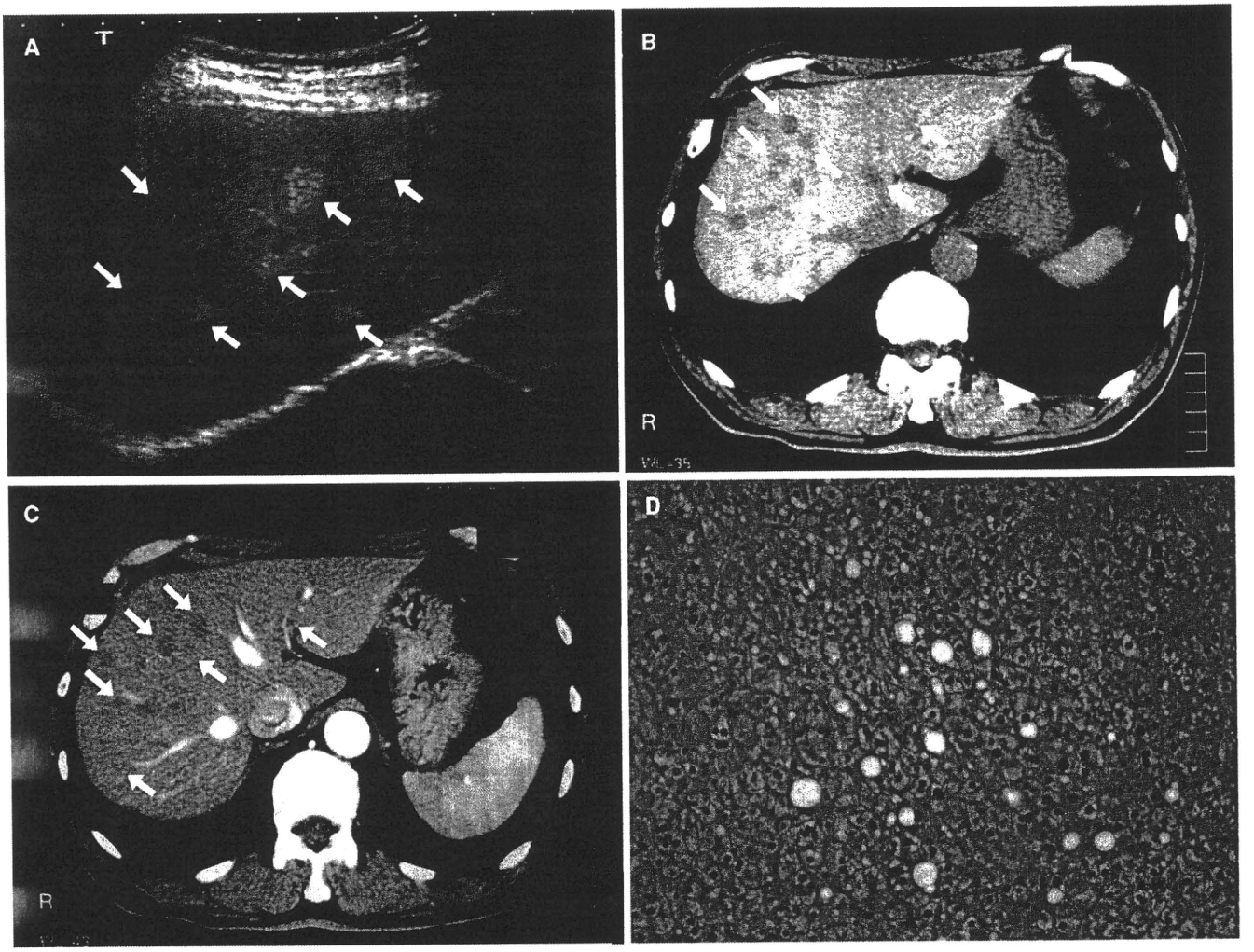

Fig. 1A–D. Diagnostic images of hepatic pseudotumors (**A–C**) and their histology (**D**). **A** Ultrasonography showing hyperechoic oval-shaped lesions. **B** Computed tomography (CT) shows multiple low-density areas spreading over the liver. **C** CT in the arterial phase of the dynamic study. Pseudotumors were slightly enhanced, but their density was still lower than that of surrounding tissues. **D** Histological image of the biopsy specimen showing slight fatty infiltration of hepatocytes

Hepatocellular carcinoma developing six and a half years after a diagnosis of idiopathic portal hypertension

To the Editor: Idiopathic portal hypertension (IPH) is a disease of unknown etiology, clinically characterized by significant splenomegaly and episodes of gastrointestinal bleeding from varices, with no liver cirrhosis or intrahepatic or extrahepatic portal obstruction.[1] Recently, nodular lesions associated with IPH have been reported, and most of these nodular lesions are hyperplastic.[2,3] However, hepatocellular carcinoma (HCC) arising in IPH is rare.[2–4] We encountered a patient with HCC that developed six and a half years after a diagnosis of IPH.

The patient was a 69-year-old woman. She had a past history of hypertension, ovariectomy due to extrauterine pregnancy with blood transfusion, obstructive hypertrophic cardiomyopathy, and diabetes mellitus. In November 1996, slight liver dysfunction, ascites, and esophageal varices were recognized. However, she did not receive further examination for liver disease. In June 1997, she was admitted to our hospital to undergo examination for liver disease. Her general status was as follows: her height was 149.5 cm, her weight was 42.5 kg, and her body mass index was 18.9 kg/m^2. She had no history of alcohol consumption. Laboratory examinations revealed mild liver dysfunction and pancytopenia. Markers for hepatitis virus and autoantibodies were all negative. We diagnosed IPH on the basis of the clinical, laboratory, radiologic, and histopathological findings (no liver cirrhosis, esophageal varices, splenomegaly, normal wedged hepatic pressure, and unknown etiology). In December 2003, when computed tomography (CT) was performed because of heart failure, a liver tumor was detected in segment 3. All tumor markers were normal, and markers for hepatitis virus were all negative. Abdominal ultrasonography (US) revealed a hyperechoic mass with a central hypoechoic area (25 × 23 mm). On CT arteriography, the mass was stained in the arterial phase with a central unstained area, and washed out on the portal phase (Fig 1a and b). On CT during arterial portography, imbalance of portal blood flow in the liver was revealed (Fig. 1c and d). By US-guided tumor biopsy, we diagnosed well-

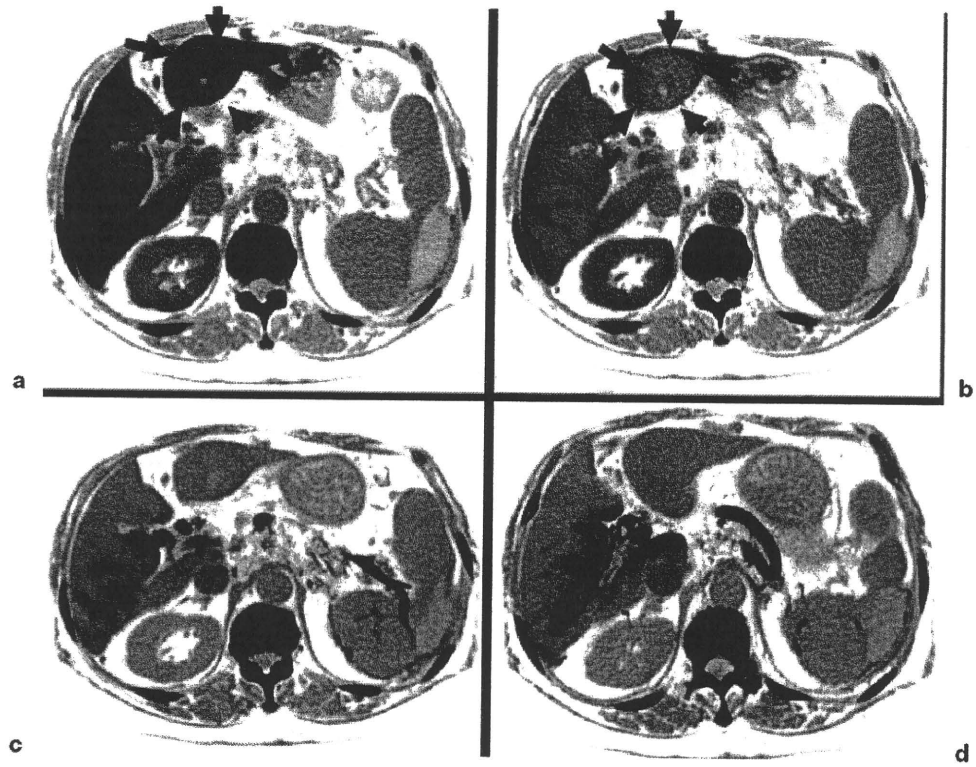

Fig. 1a–d. On computed tomography arteriography, the mass, in segment 3 (*arrows*), was stained in the arterial phase (**a**) with a central unstained area and washed out in the portal phase (**b**). An imbalance of portal blood flow in the liver was observed (**c, d**)

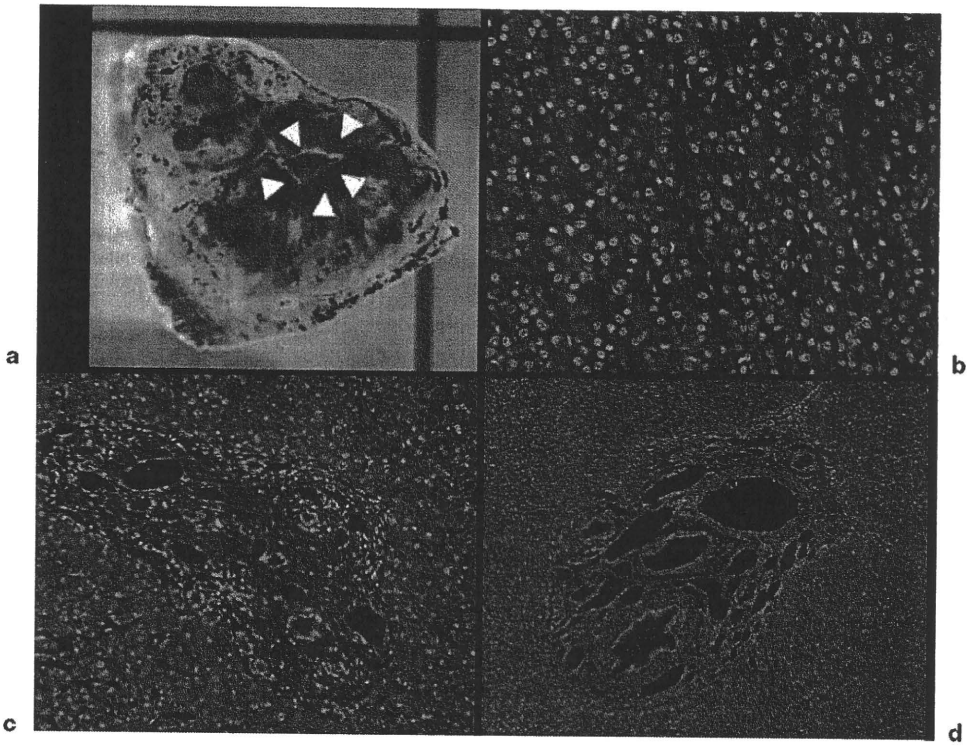

Fig. 2. a Macroscopic findings showed that the tumor had central scar-like fibrosis (*arrowheads*). **b** Histologically, the tumor was well to moderately differentiated hepatocellular carcinoma with trabecular and solid patterns. No tumorous area showed compatible idiopathic portal hypertension, but there was rounded fibrosis of the peripheral portal tracts and marked narrowing of the portal vein branches (**c**) with a thickened artery (**d**)

differentiated HCC. She underwent hepatic subsegmentectomy. Macroscopic findings showed that the tumor had central scar-like fibrosis (Fig. 2a). Histologically, the tumor was well to moderately differentiated HCC with trabecular and solid patterns (Fig. 2b). No tumorous area showed compatible IPH, which is identified by rounded fibrosis of the peripheral portal tracts and marked narrowing of the portal vein branches (Fig. 2c) with a thickened artery (Fig. 2d). After the operation, we did not find any signs of HCC recurrence. However, she died of heart failure due to obstructive hypertrophic cardiomyopathy on 25 May 2005.

Hyperplastic nodules sometimes develop in the IPH liver.[2-4] Hyperplastic nodules are attributed to abnormal blood flow in the liver due to IPH.[2] A decrease in the blood supply into the portal vein or hepatic artery could cause atrophy of the liver parenchyma, and hyperplastic changes may occur in the area where the portal blood supply increases and arterial blood supply is preserved. However, IPH patients have been considered to have a very low risk of developing HCC until now,[2-4] and the mechanisms of hepatocarcinogenesis in IPH are unknown. To our knowledge, only two patients who had HCC with IPH have been reported.[3,4]

Although HCC arising in IPH is rare, it is necessary to follow up IPH patients periodically using tumor markers and imaging modalities. Then, if tumorous lesions are detected, US-guided tumor biopsy may be necessary to diagnose malignancies because of uncharacteristic findings of imaging modalities.

Acknowledgment. The authors thank Dr. Masamichi Kojiro for the histological diagnosis of this patient.

Yumiko Isobe[1], Takahiro Yamasaki[1], Yuichirou Yokoyama[1], Fumie Kurokawa[1], Keisuke Hino[2], and Isao Sakaida[1]
[1]Department of Gastroenterology and Hepatology, Yamaguchi University Graduate School of Medicine, 1-1-1 Minamikogushi, Ube, Yamaguchi 755-8505, Japan
[2]Department of Basic Laboratory Sciences, Yamaguchi University Graduate School of Medicine, Ube, Japan

References

1. Okuda K, Kono K, Ohnishi K, Kimura K, Omata M, Koen H, et al. Clinical study of eighty-six cases of idiopathic portal hypertension and comparison with cirrhosis with splenomegaly. Gastroenterology 1984; 86:600–10.
2. Kondo F. Benign nodular hepatocellular lesions caused by abnormal hepatic circulation: etiological analysis and introduction of a new concept. J Gastroenterol Hepatol 2001;16:1319–28.
3. Hidaka H, Ohbu M, Kokubu S, Shibuya A, Saigenji K, Okayasu I. Hepatocellular carcinoma associated with idiopathic portal hypertension: review of large nodules in seven non-cirrhotic portal hypertensive livers. J Gastroenterol Hepatol 2005;20:493–5.
4. Okuda K, Nakashima T, Kojiro M, Kondo Y, Wada K. Hepatocellular carcinoma without cirrhosis in Japanese patients. Gastroenterology 1989;97:140–6.

Received: January 19, 2007 / Accepted: January 29, 2007
Reprint requests to: T. Yamasaki
DOI 10.1007/s00535-007-2025-0

529

Validating a Markov Model of Treatment for Hepatitis C Virus-related Hepatocellular Carcinoma

H. Ishida[1], J. B. Wong[2], K. Hino[3], F. Kurokawa[4], S. Nishina[5], I. Sakaida[5], K. Okita[6], T. Tamesa[7], M. Oka[7], T. Torimura[8], M. Sata[8], S. Takahashi[9], K. Chayama[9], Y. Inoue[1]
[1]Department of Medical Informatics and Decision Sciences, Yamaguchi University Hospital, Yamaguchi, Japan
[2]Department of Internal Medicine, New England Medical Center, Tufts University, Medford, MA, USA
[3]Department of Internal Medicine, Kawasaki Medical School, Kurashiki, Japan
[4]Department of Internal Medicine, Yamaguchi Rosai Hospital, Yamaguchi, Japan
[5]Department of Gastroenterology and Hepatology, Yamaguchi University Graduate School of Medicine, Yamaguchi, Japan
[6]Department of Internal Medicine, Shimonoseki Kousei Hospital, Jamaguchi, Japan
[7]Department of Digestive Surgery and Surgical Oncology, Yamaguchi University Graduate School of Medicine, Yamaguchi, Japan
[8]Department of Digestive Disease Information and Research, Kurume University School of Medicine, Kurume, Japan
[9]Department of Medicine and Molecular Science, Graduate School of Biomedical Science, Hiroshima University, Hiroshima, Japan

Summary

Objective: We created and validated a Markov model to simulate the prognosis with treatment for HCV-related hepatocellular carcinoma (HCC) for assessment of cost-effectiveness for alternative treatments of HCC.

Method: Markov state incorporated into the model consisted of the treatment as a surrogate for HCC stage and underlying liver function. Retrospective data of 793 patients from three university hospitals were used to determine Kaplan-Meier survival curves for each treatment and transition probabilities were derived from them.

Results: There was substantial overlap in the 95% CIs of the Markov model predicted and the Kaplan-Meier survival curves for each therapy. The predicted survival curves were also similar with those from the nationwide survey data supporting the external validity of our model.

Conclusions: Our Markov model estimates for prognosis with HCC have both internal and external validity and should be considered applicable for estimating cost-effectiveness related to HCC.

Keywords

Hepatocellular carcinoma, prognosis, survival rate, Markov model, validation

Methods Inf Med 2008; 47: 529–540

doi:10.3414/ME9124

1. Introduction

Hepatocellular carcinoma (HCC) is one of the most common forms of carcinoma and the incidence is increasing in Japan and other countries [1, 2]. Accordingly, the burden of HCC on health resources has risen considerably and the differences in the effect and cost of the specific treatments or periodic surveillance program for HCC has been given increasing attention.

HCCs in most cases originate from a fibrotic lesion in the liver and more than 70% of them are caused by hepatitis C virus (HCV), with some caused by hepatitis B virus (HBV) or other conditions, such as alcoholic liver injuries, in Japan [1]. Although several treatment standards for HCC have been proposed [2, 3], due to the absence of large randomized trials, the current treatment strategy for HCC remains a matter of choice, depending mostly on retrospective studies [4]. Treatments for HCC have been progressing using current technology, such as echo-guided needle insertion and catheterization into the hepatic artery. Thus, we need to establish a method to evaluate the survival benefit of each treatment. Moreover, another characteristic feature of HCC is its frequent recurrence, even after successful treatment, and the duration between a recurrence and subsequent recurrence tends to be short in the progression. These natures make it difficult to evaluate the superiority among treatments or appropriate one according to the conditions of HCC. To compensate for the lack of apparent evidence related to the treatment, a predicting prognostic computer simulation model could be a solution, but few such models for HCC that deal with the frequent recurrences and have been appropriately validated have been reported to date.

The aim of this study was to develop and validate a simulation model to predict the prognosis after initial treatments for HCV-related HCC using clinical data.

2. Method

2.1 Patients

We retrospectively studied the medical records of the patients admitted for the initial treatment of HCC between January 1994

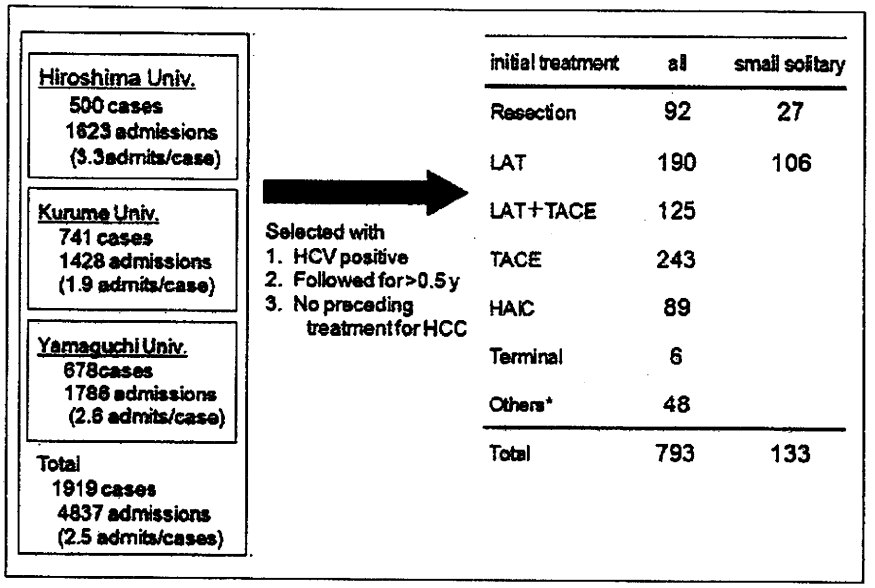

Fig. 1 Retrospective survey of HCC cases among three universities. * Others included combination of three treatment, combination of resection and LAT, and combination of resection and TACE.

and December 2003 at the three university hospitals; Yamaguchi, Hiroshima and Kurume. Total subjects were 1913 cases with 4837 admissions (Fig. 1).

The inclusion criteria were naïve HCV-related HCC cases with a follow-up period of more than half a year after the first admission. Total of 793 patients were eligible. They had an average 3.1 admissions (range: 1-17) and were followed for an average of 37 months (range: 181-3920 days). Among these patients, initial treatment by hepatic resection (HR), local ablation therapy (LAT), combination therapy of LAT and transcatheter arterial chemoembolization (TACE), TACE monotherapy, hepatic artery infusional chemotherapy (HAIC) or systemic chemotherapy and supportive treatment for terminal state were indicated for 92, 190, 125, 243, 89 and 6 patients respectively.

The average age of the patients was 64.7 years old (range: 40-83), male ratio was 0.62 and the proportion of liver cirrhosis was 0.89. The other characteristics were presented in Table 1. They were maximal size and number of tumors, the proportion of cases with previous history of interferon therapy, ratio of involvement with portal vein, hepatic artery or vein, or biliary duct, vascularity of tumor, total follow-up period, average number of admission and number of attained complete remission state and duration of it. Limiting the population to solitary and small tumors (less than 3cm in maximum diameter) as an early HCC state,

Table 1 Baseline characteristics of the cases

Initial treatment		HR (N = 92)		LAT (N = 190)		LAT + TACE (N = 125)		TACE (N = 243)		HAIC (N = 89)		Terminal (N = 6)		Others* (N = 48)	
		Mean	SD	Mean	SD	Mean	SD	Mean	SD	Mean	SD	Mean	SD	Mean	SD
Age		63.4	8.3	66.2	8.3	66.5	7.7	65.8	7.4	65.6	6.3	62.7	11.9	66.4	8.0
Male ratio		0.83		0.64		0.67		0.70		0.81		0.67		0.75	
Tumor	Max. size	3.99	2.79	2.18	2.69	2.36	1.03	3.88	2.72	5.10	3.53	4.05	2.32	3.08	2.36
	Number**	1.71	1.35	1.52	0.89	2.31	1.91	3.04	2.91	6.16	6.08	2.83	1.60	2.83	2.21
IFN treatment before admission (rate)		0.23		0.14		0.11		0.06		0.05		0.00		0.16	
Involvement of vessels (rate)		0.23		0.05		0.02		0.14		0.27		0.33		0.19	
High vascularity of tumor (rate)		0.92		0.72		0.89		0.97		0.99		0.83		0.93	
Total FU*** (day)		1339	862	1255	866	1309	815	1026	770	682	529	404	295	1243	891
No. of admission		2.28	1.95	2.87	2.08	3.85	2.28	3.41	2.03	2.13	1.44	1.67	0.52	3.46	2.74
No. of CR#		1.27	0.76	1.29	0.98	1.08	1.14	0.67	0.94	0.37	0.77	0.00	0.00	0.58	0.85
CR duration (day)		922	836	709	691	501	598	359	626	142	351	0	0	287	488
CR	Rate/admission	0.71	0.36	0.56	0.38	0.32	0.33	0.22	0.31	0.16	0.31	0.00	0.00	0.20	0.31
	Duration/total FU	0.68	0.34	0.55	0.36	0.33	0.33	0.25	0.35	0.13	0.28	0.00	0.00	0.22	0.33

* include combination of three treatments, combination of resection and LAT, and combination of resection and TACE
** In case that more than ten nodules were seen, its number of tumors was treated as 11 nodules.
*** follow-up periods
# complete remission after treatment

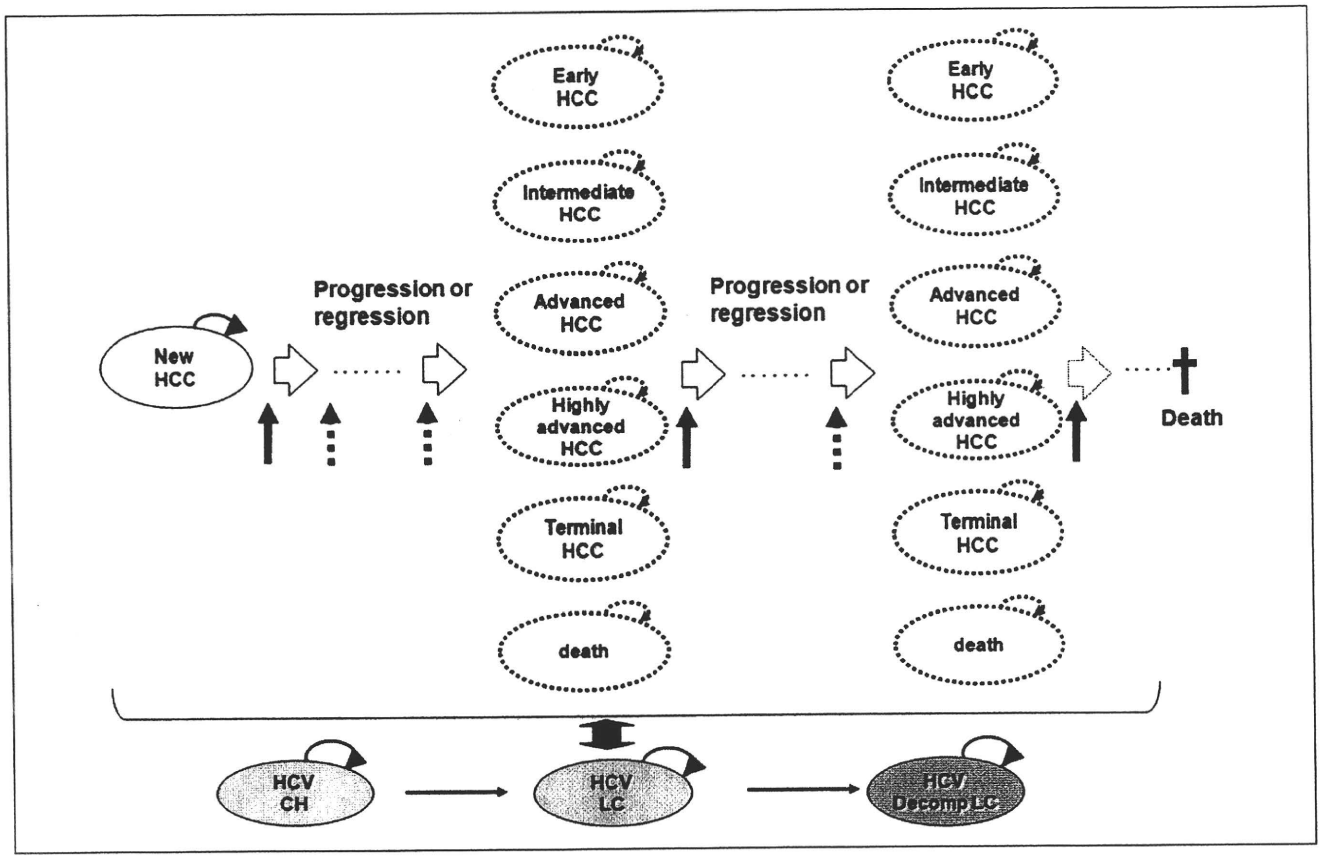

Fig. 2 Schema of the Markov model of treatment for HCC. Solid vertical arrows indicate optimal treatments according to HCC characteristics and preserved liver function, and dashed vertical arrows indicate the same treatments undertaken optionally for the same state of HCC. Outlined horizontal arrow indicates a Markov cycle representing progression or regression from one state to another at a constant transition probability in each cycle. Along with the transition of HCC state, underlying chronic hepatitis caused by HCV may also progress to a more advanced cirrhotic state.

we evaluated 27 of HR and 106 of LAT cases.

2.2 Development of a Markov Model According to Treatment Strategy

We developed a Markov model to predict prognosis of HCC patients to whom the different initial treatment options were indicated according to the tumor characteristics and preserved liver function. The Markov model is a multistate transition model that allows patients in a hypothetical cohort to make transitions among various health states, at different rates, over extended periods. In our model, the health states of treatment were represented as states of the Markov process. The schema of the Markov model (Fig. 2) represented possible transitions after initial treatment of HCC, and duration of each cycle was one-month. Figure 3 showed the model as a decision tree in which treatment arms were listed at the decision node and health states emanated from the Markov node. Once a patient entered the models the state of HCC might progress to a more advanced one by aggravation of HCC or regress to an improved one by efficient treatment, and also, underlying chronic hepatitis (CH), compensated liver cirrhosis (LC) or decompensated LC (decLC) might develop more advanced liver disease.

All Markov states led to the Markov subtree in a Markov cycle of one month (Fig. 4). The model consisted of two parts; one part was the initial HCC state that indicated the optimal treatment, and the other was the subsequent recurrence states. We defined the same HCC state that remained in the same condition or the status of complete remission, and the different HCC state that changed to another state due to recurrence or death from liver disease. We did not consider a direct treatment effect that is clinical judgment whether or not tumors were totally removed (complete remission). The reason is that it is not always possible to determine complete remission accurately.

2.3 Model Assumptions

Our model assumed that each optimal treatment was selected according to the tumor characteristics, such as size, number and existence of invasion to the portal vein,

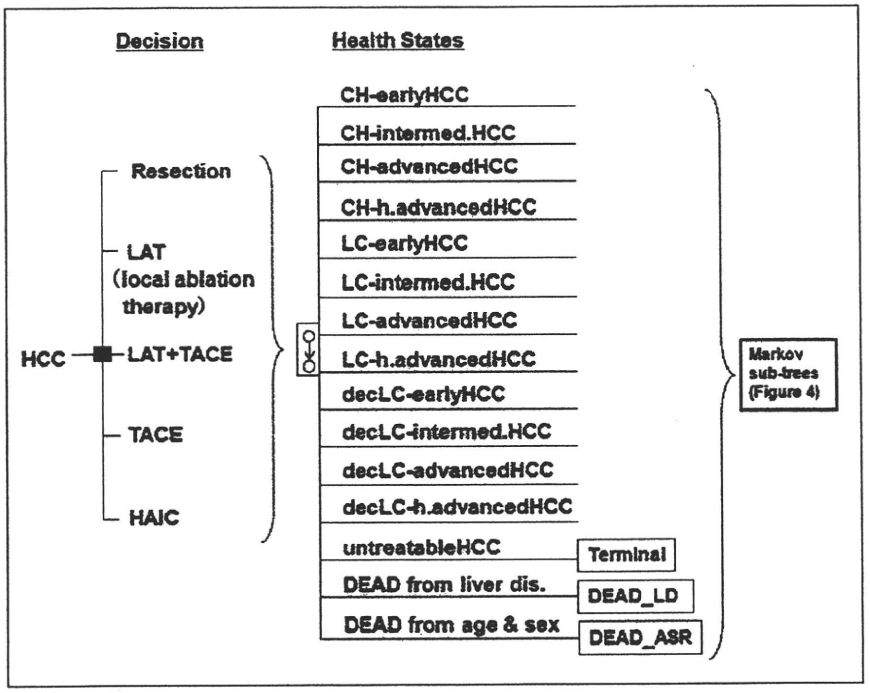

Fig. 3 Structure of decision tree with Markov process. Solid square indicates decision node of therapeutic procedures followed by Markov node (a rectangle with circles connected by an arrow) including 15 HCC (health) states. intermed.: intermediate, h.advanced: highly advanced

hepatic vein or biliary duct, and underlying liver state. In our treatment strategy, hepatic resection or LAT would be selected for the early HCC state (in general, small and solitary or oligo-nodules), combined therapy with LAT and TACE for the intermediate HCC state, TACE monotherapy for advanced HCC state, HAIC or systemic chemotherapy for highly advanced HCC state and supportive therapy for a terminal HCC state, respectively. In addition, the following assumptions were incorporated into the model.

1) The progression of underlying liver disease, such as CH to LC, LC to decLC, decLC to death occurs unrelated to the HCC state and the effect of treatment for HCC.
2) Patients in the HR groups undergo HR up to two times and they are subsequently eligible for LAT in case of early HCC.
3) In the case with decompensated liver cirrhosis, hepatic resection should not be selected, even for small solitary HCC, but LAT might be selected if preserved liver function would be tolerable.
4) Liver transplantation for HCC or decompensated liver cirrhosis was not incorporated into the model because such cases were so few in our data
5) We did not consider death caused by CH or compensated LC, except for the mortality rate for the general population by age and sex.

2.4 Estimation of Transition Probabilities and Rates of Next States

The length of transition of any HCC state was defined as the period from the date of admission for the treatment of some HCC state to the date of next admission for the different HCC state or to the date of death (Fig. 5).

The monthly transition probabilities were estimated separately by the cases from the group of initial treatment, and those from the group of recurrences. We obtained the median transition periods by nonparametric Kaplan-Meier (KM) method by treating transitions to different states including death related to liver disease as events data, and death unrelated to liver disease or withdrawal from follow-up as censored data. The median transition period was then converted into a monthly transition probability using the DEAL method [5, 6].

The rate of the next health state was calculated by the number of the state divided by the total number of the subsequent different states.

The transition probability of the terminal state to death was assigned equally, unrelated to underlying liver disease or HCC state, in which it was not possible to undergo any treatment for HCC, but only supportive therapy.

2.5 Progression of Underlying Liver Disease and Treatment-related Mortality

The annual progression rates from CH to compensated LC and compensated LC to decompensated LC were assigned values of 0.073 and 0.06, respectively, based upon previous studies [7].

Though we identified no case died within one month after any therapeutic procedure, we assigned the direct mortality rates caused by treatment procedure to be 0.008 for HR from the report of nationwide follow-up survey of primary liver cancer in Japan [8] and 0.001 for other treatments by experts' opinion.

2.6 Cohort Simulation

We analyzed the prognosis after initial therapy for the two categories of HCC cases as follows.

1) Early HCC cases (solitary and small tumor) that underwent hepatic resection or LAT.
2) Non-early cases that selected the combination therapy of LAT and TACE (LAT+TACE), TACE monotherapy or HAIC as the optimal initial treatment.

The simulation cohort had the same characteristics as the actual cases. The start age of the simulation was 65 years old, male ratio was 0.62 and the LC ratio was 0.89.